

# Characteristics of Ant-Inspired Traffic Flow

## Applying the social insect metaphor to traffic models

Alexander John<sup>1</sup>, Andreas Schadschneider<sup>1,2</sup>, Debashish Chowdhury<sup>3</sup>, Katsuhiko Nishinari<sup>4</sup>

<sup>1</sup> Institut für Theoretische Physik, Universität zu Köln, 50937 Köln, Germany

<sup>2</sup> Interdisziplinäres Zentrum für komplexe Systeme, Bonn, Germany

<sup>3</sup> Department of Physics, Indian Institute of Technology, Kanpur 208016, India

<sup>4</sup> Department of Aeronautics and Astronautics, Faculty of Engineering, University of Tokyo, Tokyo, 113-8656, Japan

Received: date / Revised version: date

**Abstract** We investigate the organization of traffic flow on preexisting uni- and bidirectional ant trails. Our investigations comprise a theoretical as well as an empirical part. We propose minimal models of uni- and bidirectional traffic flow implemented as cellular automata. Using these models, the spatio-temporal organization of ants on the trail is studied. Based on this, some unusual flow characteristics which differ from those known from other traffic systems, like vehicular traffic or pedestrians dynamics, are found. The theoretical investigations are supplemented by an empirical study of bidirectional traffic on a trail of *Leptogenys processionalis*. Finally, we discuss some plausible implications of our observations from the perspective of flow optimization.

### 1 Introduction

Traffic-like problems are relevant in various biological systems ranging from the motion of motor proteins in cells on a microscopic scale [14, 8] to the behavior of social insects on a macroscopic scale [4, 3, 10, 11]. This has led to the development of various models that try to explain the collective behavior observed empirically in these systems. Besides their interesting transport properties, colonies of social insects can be seen as multi-agent systems, facing and solving various kinds of problems [9, 10, 11]. For that reason the social insect metaphor has already been employed with great success in computer science [1, 2]. This can also be extended to other fields, for example models of pedestrians dynamics where the concept of chemotaxis [15, 13] has

been adopted for incorporating the mutual interactions of pedestrians [26]. A 'virtual chemotaxis' mechanism allows these models to reproduce the collective phenomena observed empirically in the dynamics of large crowds. In addition, also effects arising from the direct coupling of counterflowing streams of pedestrians or ants have been subject of extensive empirical as well as theoretical investigations [27, 10, 11, 19].

Taking into account these basic aspects, which will be addressed in more detail below, minimal particle-hopping models for traffic flow on preexisting uni- and bidirectional ant trails have been proposed [7, 17, 16]. These models are implemented as cellular automata that have been previously used to successfully describe traffic flow in various other fields, e.g. physical systems [5] like surface growth and human transport systems on highways and in cities [25, 6].

The main focus of the present work consists in the proposal of very basic and hence quite general models. We identify the main features of the flow-density relation of already established trails and present simulation results for the proposed models in the full parameter regime of attainable densities.

In addition to the theoretical considerations, we present the first empirical traffic data from a bidirectional trail of *Leptogenys processionalis*. In order to facilitate the comparison with the predictions of the simplified models, the proposed experimental setup, that is the choice of the ant species and of the type of trail, has to satisfy certain restrictions. In order to reduce complexity, we observed traffic flow of a monomorphic species on a preexisting trail. More details will be given in Sec. 4 and in the subsequent discussion.

Nevertheless, the techniques employed might also apply in a more general setup. The data obtained this way are compared with previous empirical results [4, 3, 21] and give some indications for more realistic extensions of the minimal models studied here which focus only on some key features of ant traffic (additional aspects related to non-equilibrium physics or the application to pedestrian dynamics are treated in [20, 19]).

## 2 The unidirectional model

The model for unidirectional flow that we have introduced in [7] and that will be considered further in this paper can be seen as an extension of the so-called totally asymmetric simple exclusion process (TASEP) [28, 6], a well studied model in non-equilibrium physics. Ants will be modelled by particles<sup>1</sup> that move stochastically along a one-dimensional lattice. In the following, we define the TASEP and then certain extensions are added that lead to the unidirectional ant trail model that we propose in this paper. In a further step the unidirectional model will be extended to the bidirectional one.

---

<sup>1</sup> In the following we will use the terms ant and particle interchangeably.

### 2.1 TASEP regime

The TASEP is defined by a simple set of rules. Particles (representing the ants) hop in a fixed direction from one lattice-site  $i$  to the next one  $i + 1$ . Each site can be occupied only by one particle (exclusion principle). Time evolution is continuous, which can be realized by a random-sequential update scheme: In each update step, one site  $i$  is chosen at random. If site  $i$  is occupied and  $i + 1$  is empty, hopping takes places with probability  $q$ . If site  $i + 1$  is blocked by another particle, nothing happens (exclusion principle) and another site is chosen randomly. A particle leaving the last site  $L$  will hop to site 1, i.e. motion takes places in a ring geometry. More realistic geometries are possible, but the main effects in our models are quite robust against a change of boundary conditions [22].

One important way of characterizing a traffic-like system is the fundamental diagram [23]. It relates the average velocity  $V$  or the flow  $F$  with the density  $\varrho$  of agents in the system. Both relations  $F(\varrho)$  and  $V(\varrho)$  are equivalent due to the hydrodynamic relation  $F = \varrho V$ . Nevertheless, both will be used in the following since certain features can be seen more clearly using the average velocity, other using the flow.

In the TASEP with random-sequential dynamics and  $N$  particles hopping on a lattice with  $L$  sites, flow  $F$  and average velocity  $V$  as a function of density  $\varrho$  are exactly given by (see e.g. [28, 6])

$$V(\varrho) = q(1 - \varrho), \quad F(\varrho) = q\varrho(1 - \varrho) \quad \text{with} \quad \varrho = \frac{N}{L}. \quad (1)$$

Mutual blocking of particles is the only mechanism of interaction, leading to a strictly monotonic decrease of average velocity with increasing density. Flow and average velocity are directly linked to the spatio-temporal distribution of particles. The density  $\varrho$  gives the probability of finding a particle at a site  $i$ , whereas  $1 - \varrho$  gives the probability of finding a particular site being unoccupied. The distribution of particles is homogeneous on time-average. Due to increased mutual blocking the average velocity decreases strictly monotonically with increasing density, which agrees with the behavior found for example in vehicular traffic [23, 6].

### 2.2 Cluster regime

The model for unidirectional ant trails [7] is obtained by extending the TASEP. Now each lattice site can also be occupied by a pheromone-mark and/or one ant (see Fig. 1 left). If a pheromone mark but no ant is present at site  $i + 1$ , an ant at site  $i$  will hop to site  $i + 1$  with probability  $Q$ . If neither an ant nor a mark are present, hopping will take place with probability  $q < Q$ . Also pheromones evaporate: if one site is marked but no particle is present, this mark will be removed (evaporated) with probability  $f$ . If a particle is present and the site is chosen for updating, the mark will not

evaporate, reflecting the reinforcement of the pheromone-mark by the ants. The corresponding probability  $p(i, \Delta t)$  of finding a pheromone at site  $i$  is therefore given by

$$p(i, \Delta t) = \begin{cases} 1 & \text{if } i \text{ is occupied} \\ (1 - f)^{\Delta t} & \text{else} \end{cases} \quad (2)$$

where  $\Delta t$  is the time-interval between the occupation of a site  $i$  by two succeeding ants, called time-headway in traffic engineering. Obviously the time-headway determines the decay of the probability of finding a pheromone.

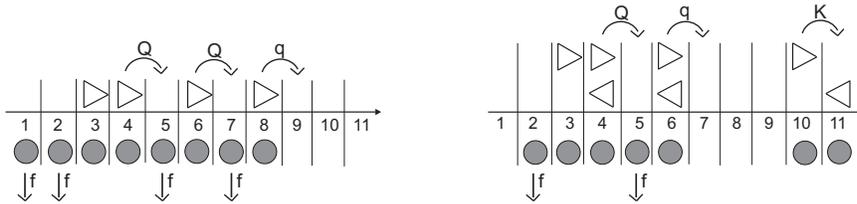


**Fig. 1** Definition of the uni- (left) and bidirectional model (right): The symbols correspond to particles (representing ants) moving to the right ( $\triangleright$ ), particles moving to the left ( $\triangleleft$ ), and pheromone marks ( $\bullet$ ). Although a natural trail is two-dimensional, the ant motion can be considered to be one-dimensional allowing to map the trail onto a one-dimensional lattice with  $L$  sites. Particles move stochastically along the lattice, with hopping rates  $q$  and  $Q$ . Free pheromones can evaporate with rate  $f$ . Java applets illustrating the dynamics of the models can be found at [www.thp.uni-koeln.de/~aj](http://www.thp.uni-koeln.de/~aj).

In the case  $f = 0$  ( $f = 1$ ) pheromones will never (immediately) evaporate and the TASEP-case with hopping probability  $Q$  ( $q$ ) is recovered (Fig. 2). More interesting properties arise in case of  $0 < f < 1$ . The most surprising feature is the non-monotonic dependence of the average velocity on density for small evaporation rates  $f$  (Fig. 2 left).

At low to intermediate densities, the average velocity stays constant ( $V = q$ ). Beyond a certain threshold value a sharp increase of velocity can be seen. In the regime of high densities, the monotonic decrease known from the TASEP is found. Both regimes are a consequence of the incorporation of pheromone marks. Each ant is followed by a trace of marks (Fig. 3 middle). A succeeding ant perceiving this trace will hop with probability  $Q > q$ . If the preceding particle sees no pheromone mark, it will hop with probability  $q < Q$ . Then faster ant will catch up with the slower ones forming a moving cluster (see Fig. 3 middle and Fig. 3 right). Similar results are known from systems with particle-wise defects [18] where each particle  $j$  has its own individual hopping probability  $q_j$ . Here also clusters are formed and the average velocity stays constant  $v = q$ . An example from vehicular traffic is a platoon of cars following a slow truck. At very low evaporation rates

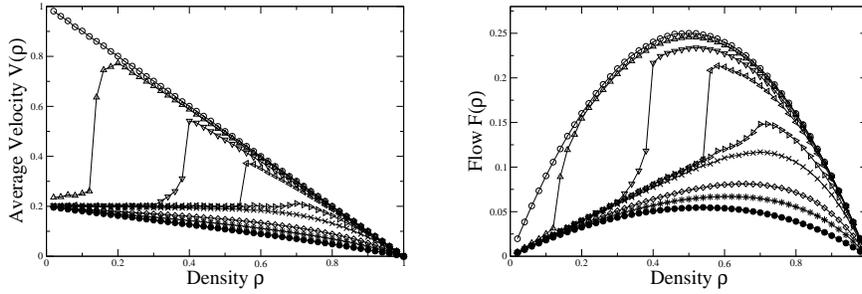


**Fig. 2** Fundamental diagrams for the cellular automaton implementation of the unidirectional model:  $Q = 0.9$ ,  $q = 0.2$  and  $f = 0(\circ)$ ,  $0.0002(\Delta)$ ,  $0.0008(\nabla)$ ,  $0.002(\triangleleft)$ ,  $0.008(\triangleright)$ ,  $0.02(\times)$ ,  $0.08(\diamond)$ ,  $0.2(*)$ ,  $1(\bullet)$ . In case of  $f = 1$  and  $f = 0$  the average velocity  $V(\rho)$  and flow  $F(\rho)$  are exactly known from the TASEP. At low to intermediate densities, the average velocity stays constant for a suitable choice of evaporation probability  $f$ .

or at high densities (small average distance or distance-headway), all ants perceive pheromone marks. So on average their hopping probabilities all reach the same value  $Q$ , leading to TASEP-like features. The corresponding distribution of ants becomes homogeneous (see Fig. 3 left).

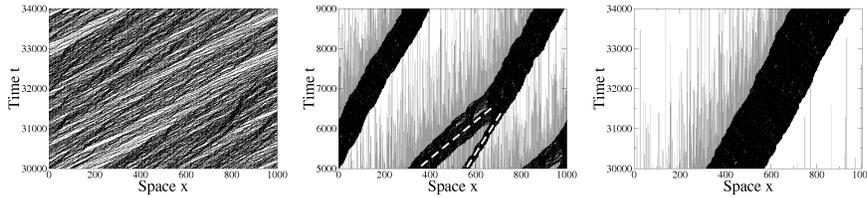


**Fig. 3** Space-time plots for the unidirectional model:  $Q = 0.9$ ,  $q = 0.2$ ,  $f = 0.001$ ,  $\rho = 0.2$ . On the left the TASEP case ( $p = 0.9$ ) is shown. Besides fluctuations, particles are distributed randomly. The other two plots show different stages of the cluster formation in the unidirectional ant trail model. Each ant (black) is followed by a trace of pheromones (grey). Due to evaporation this trace has a finite length. As indicated by the different slopes of the ants trajectories (middle) clusters move with different velocities depending on the presence of pheromones. Finally, in the stationary state only one moving cluster survives (right).

### 2.3 A comparison with models of vehicular traffic

As already mentioned, cellular automaton models are well established in case of vehicular traffic [6]. They seek to capture the complex behavior of a system composed of humans driving in their cars. Besides certain similarities, models of ant traffic should also reflect crucial differences to vehicular

traffic. One is the lack of some kind of velocity memory. In our model, ants reach their walking speed within one single update step. This is similar to the motion of pedestrians where the walking speed is also reached within a time less than 1 sec. In contrast, in vehicular traffic cars cannot accelerate instantaneously to the maximum velocity and so velocity is only increased gradually [25,26,6].

Furthermore, the behavior of ants can be expected to be much more homogeneous than that of drivers on a highway. Here a mixture of different vehicles with different maximum speeds, acceleration capabilities, and so on, but also of different kinds of drivers with different moods or attitudes, influences the overall behavior [23]. Therefore, the range of possible velocities in vehicular traffic can be assumed to be larger than in ant traffic, at least in comparison with monomorphic species. As a consequence of the speed homogeneity, overtaking is rarely observed on ant trails at least under certain conditions [16] and has therefore not been included into our model.

Also the definition of the update procedure itself can have a strong influence on the dynamics. For modelling vehicular traffic a time-parallel update is widely used which performs a synchronous update of all lattice sites [6]. As only the occupation of the lattice at the moment of updating is used, a synchronous update incorporates time latencies of the drivers. But in case of ants the perception range is limited to their immediate environment [13,24,15] and the random-sequential update described above is more appropriate.

The stochasticity in the model has mainly two sources. First, many influencing factors are not known or difficult to include explicitly since the model would become too complicated. Thus they are included in a statistical sense through probabilities for a certain behavior. The second reason lies in the behavior of the ants themselves. They appear to possess an intrinsic stochasticity depending on the evolution of the particular species [13]. This is also widely used in applications [1,2]. In vehicular traffic stochasticity is used to incorporate fluctuations in the driver's behavior which can lead to spontaneously formed phantom jams [25].

### 3 The bidirectional model

For extending the unidirectional model to the case of bidirectional flow we have investigated several models [19,17]. As one common requirement they should reduce to the unidirectional model in case of vanishing counterflow. In the extension discussed here another lattice for ants moving in the opposite direction is added (see Fig. 1 right). Both lattices for ants obey the same set of dynamical rules. An extension to multiple lanes is then straightforward by adding further one-dimensional lattices. Experimental studies already addressed this issue [9,3]. Going further one could consider the extension to a two-dimensional model. Here the trail topology including the formation of lanes itself could be incorporated more naturally. Especially the relation between flow properties and trail topology could be investigated. Also the

analogies to already existing models of pedestrians dynamics surely provide a fruitful perspective [26,27].

Overall, one deals with three hopping probabilities depending on the occupation of the nearest neighboring site in hopping direction. In absence of counterflow again the rates  $q$  and  $Q$  apply. In case of counterflow one additional rate  $K$  (see Fig. 1 right) is used. This is a crucial difference to most models of vehicular traffic which usually neglect the coupling of lanes in opposing directions [6]. Workers facing each other in opposite directions have to slow down due to information exchange or just in order to avoid collision [4,3,9,11]. Therefore, we choose hopping probabilities satisfying  $K < q < Q$ .

A related problem is the organization of ant traffic at bottlenecks. For *Lasius niger* this has already been investigated experimentally [11]. In that case traffic flow is organized such that the number of encounters inside the bottleneck is reduced. This is quite different from our bidirectional model where the main effect originates from these head-on encounters (see Fig. 9 right). Here some similarities to models of pedestrians dynamics can be drawn [27,19]. Under crowded conditions separated lanes for each direction are formed dynamically. These lanes are stabilized by incorporating the desire of pedestrians to reduce the number of encounters with others in the counterflow.

### 3.1 Equal densities

In general, the fundamental diagram can be expected to depend on both densities  $\rho_L$  and  $\rho_R$  of left- and right-moving ants. That is, it has the form  $F = F(\rho_L, \rho_R)$ . For simplicity, we start the discussion with equal densities in both directions. Finally, we investigate the full fundamental diagram focusing on the generic properties and differences to the other cases.

*3.1.1 Cluster regime* The average velocity roughly shows the behavior already known from the unidirectional case (see Fig. 2 left), including the anomalous density dependence (see Fig. 4 left). As the average lifetime of the pheromone marks is determined by the mean distance-headway (mean ant-ant distance) of ants in both directions, this regime only exists at very low densities. Similarly to the strictly unidirectional case, moving clusters for each direction are formed (see Fig. 5 left). With increasing density the lifetime of the pheromone marks increases such that they become present at every site and thus suppressing the mechanism of cluster formation.

*3.1.2 Plateau regime* The generic property of this model is found in flow and cannot be observed directly in the average velocity [17,16]. For all values of  $f$ , flow roughly stays constant over a certain density regime (see Fig. 4 right). Due to the behavior of the average velocity one observes a shift of the beginning of the plateau in flow to lower densities with decreasing

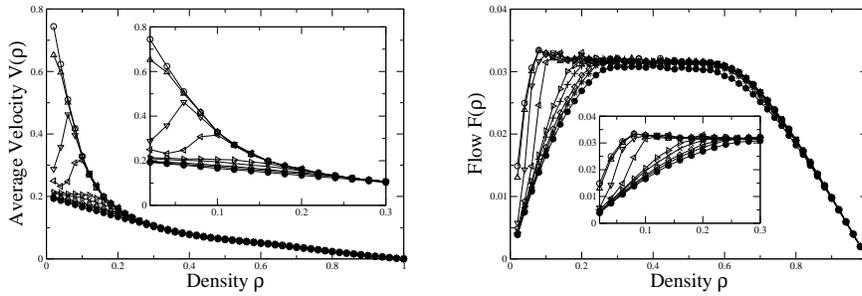


**Fig. 4** Fundamental diagrams for the cellular automaton implementation of the bidirectional model:  $Q = 0.9$ ,  $q = 0.2$ ,  $K = 0.1$  and  $f = 0(\circ)$ ,  $0.0002(\triangle)$ ,  $0.0008(\nabla)$ ,  $0.002(\triangleleft)$ ,  $0.008(\triangleright)$ ,  $0.02(\times)$ ,  $0.08(\diamond)$ ,  $0.2(*)$ ,  $1(\bullet)$ . The average velocity shows the same non-monotonicity already observed in the unidirectional model. The main property of the bidirectional model is exhibited by flow. For intermediate densities the flow is nearly independent of the density  $\rho$  and the evaporation rate  $f$ .

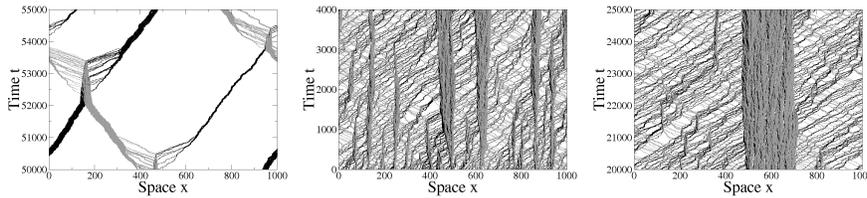


**Fig. 5** Space-time plots for the cellular automaton implementation of the bidirectional model:  $Q = 0.9$ ,  $q = 0.2$ ,  $K = 0.1$ ,  $f = 0.002$ . The left plot shows the formation of small moving clusters for  $\rho_L = \rho_R = 0.03$ . One observes one left-moving (grey) and two right-moving clusters (black). With increasing density this regime vanishes as the pheromones are present at any site. Due to the coupling to counterflow a large localized cluster emerges (plotted for  $\rho_L = \rho_R = 0.2$  in the middle and on the right).

$f$ . But at intermediate to high densities, there is obviously no dependence on  $f$ . This effect originates from the mutual hindrance by counterflowing ants. Similar effects are known from systems with lattice-wise disorder [29] where the hopping probabilities depend on the actual position (e.g., due to construction works or car accidents in vehicular traffic). In our case we find several localized clusters of ants in both directions (see Fig. 5 right). They form some kind of dynamically induced defects, as ants facing these clusters move with reduced hopping probability  $K$ .

### 3.2 Different densities

For natural trails, different densities  $\rho_R$  and  $\rho_L$  for each direction are more realistic. Ants moving back to the nest might be carrying load and there-

fore will behave quite differently from outbound ants [4, 9, 12]. More complex models could incorporate this by also employing different hopping rates depending on the direction. But here we consider only symmetric hopping rates and focus on right-moving ants, treating the left-moving ones as counterflow. This is no restriction due to the symmetry

$$F^R(\rho_L, \rho_R) = F^L(\rho_R, \rho_L) \quad (3)$$

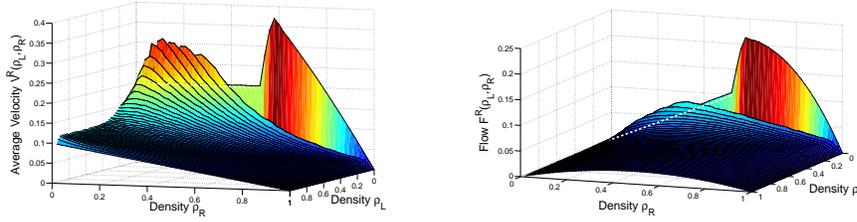


**Fig. 6** Fundamental diagrams for the full bidirectional model. Average velocity  $V^R(\rho_L, \rho_R)$  and flow  $F^R(\rho_L, \rho_R)$  are shown for the full range of densities  $(\rho_L, \rho_R) \in [0, 1] \times [0, 1]$ . In case of vanishing counterflow ( $\rho_L = 0$ ) obviously the unidirectional case is recovered.

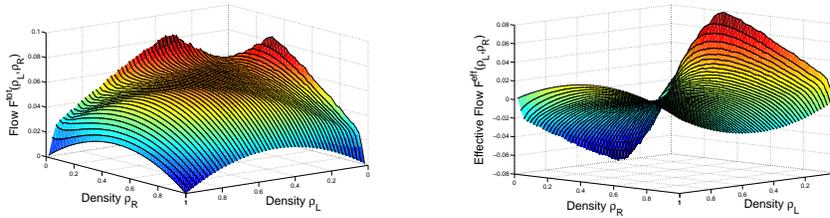


**Fig. 7** Extended fundamental diagrams for the full bidirectional model. Total flow  $F^{\text{tot}}(\rho_L, \rho_R)$  and effective flow  $F^{\text{eff}}(\rho_L, \rho_R)$  are shown for the full range of densities  $(\rho_L, \rho_R) \in [0, 1] \times [0, 1]$ . Symmetries according to (4) and (5) are found. For clarifying the generic features due to counterflow, the limiting cases  $\rho_R = 0$  and  $\rho_L = 0$  are not shown.

*3.2.1 Properties of the full fundamental diagram* The behaviour of the average velocity shows strong deviations from the characteristics of strictly unidirectional flow (see Fig. 6 left). Obviously, the regime of constant velocity only exists for a small area in the  $\rho_L, \rho_R$ -plane. Although counterflow leads to a reduced hopping rate  $K$ , the average velocity is even increased

by counterflow. As already observed for the special case of equal particle numbers, a non-monotonicity is found at very low densities  $(\rho_L, \rho_R) \in ]0, 0.1] \times ]0, 0.1]$ . For larger densities, a strictly monotonic decrease is found. As a result, the average velocity in case of counterflow is lower than for strictly unidirectional flow ( $\rho_L = 0$  or  $\rho_R = 0$ ). Overall, the observed feature is rather an effect of the shared pheromone lattice than of the reduced hopping rate due to counterflow. As pheromones become present at nearly any site, no particle-wise disorder can be induced anymore. Therefore a quasi-TASEP case is attained in which the impact of counterflow can be neglected. With increasing density of counterflowing ants the impact of pheromones vanishes and hopping predominantly takes place with rate  $K$ . As already observed in the special case  $\rho_L = \rho_R$ , flow reaches a nearly constant value (see Fig. 6 right).

*3.2.2 Additional quantities of interest* Total and effective flow are non-zero quantities in case of different particle numbers or hopping rates for both directions. The total flow  $F^{\text{tot}}(\rho_L, \rho_R)$  measures the total number of moving ants per unit time and is independent of the direction of movement. For quantifying the effective number of ants moving in one particular direction the corresponding flow  $F^{\text{eff}}(\rho_L, \rho_R)$  is used:

$$F^{\text{tot}}(\rho_L, \rho_R) = F^R(\rho_L, \rho_R) + F^L(\rho_L, \rho_R) = F^{\text{tot}}(\rho_R, \rho_L), \quad (4)$$

$$F^{\text{eff}}(\rho_L, \rho_R) = F^R(\rho_L, \rho_R) - F^L(\rho_L, \rho_R) = -F^{\text{eff}}(\rho_R, \rho_L). \quad (5)$$

As a consequence of employing the same set of hopping rates for both directions, the quantities exhibit different kinds of symmetries due to (3). One also observes plateaus which are a consequence of the plateaus found in  $F^R$  and  $F^L$  for an intermediate range of densities  $(\rho_L, \rho_R)$  (see Fig. 7). Both features might be subject of first qualitative empirical investigations. The total flow might be of interest especially in the ecological context of collective transport like foraging [4, 3] since it measures the total performance of the employed foraging strategy, in contrast to the effective flow. On the other hand, the latter allows to identify the overall direction of movement.

#### 4 A brief outlook to empiricism

The discussed analogies between ant- and vehicular traffic can also be used for experimental investigations. Based on this we collected qualitative and quantitative traffic data [16]. As our models are quite simple, the experimental setup, as well as the observed species, have to meet some well defined requirements. The observed trail section has to exhibit a constant shape for the period of data collection which is the equivalent of a static road. To minimize complexity, intersections or branchings are excluded. These would be analogous to on- and off-ramps which are known to have a strong influence on vehicular traffic [6, 23]. As already pointed out (see Sec. 2.3) the moving agents in both systems can be assumed to be quite different. For our

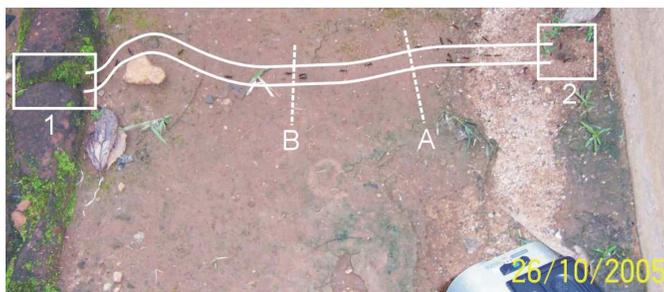


**Fig. 8** Illustration of the experimental setup. The observed section A-B used for data extraction is located in the middle of the bidirectional trail. A narrow passage on the left leads to a huge lawn (framebox 1). On the right the entrance to the nesting site can be seen (framebox 2).

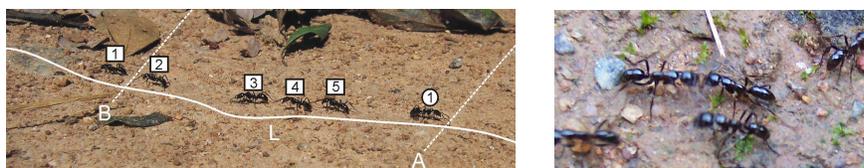


**Fig. 9** Illustration of the observed section. Ants following the established trail leave the observed section in the same order of entering (left). Therefore the  $n$ -th ant entering will also be the  $n$ -th one leaving. Counting is done separately for each direction. Ants facing each other in opposite directions slow down in so-called head-on encounters (right).

investigations we chose ants of the monomorphic species *Leptogenys processionalis*. The analogy in vehicular traffic would be a traffic flow composed out of many copies of the same car driven by nearly the same driver. This choice ensures that all moving agents are basically equivalent at least for each direction of movement. Especially no laden ants were observed.

#### 4.1 Methods

The field studies were performed on the campus of the *Indian Institute of Science, Bangalore, India*. We obtained qualitative as well as quantitative data for one bidirectional single lane trail which was observed for about 25 minutes. Similar investigations have been made for ten other trails of the same type which have been found to exhibit the same qualitative and quantitative properties. The criteria employed for the choice of the trails are for example the trail topology (single-lane, bidirectional) or the observed means of interaction (e.g., head-on encounters). Particular features will be addressed in more detail in the subsequent discussion.

*4.1.1 Basic quantities and observations* For collecting quantitative data we chose a relatively small section located in the middle of the trail (Fig. 8) to reduce additional effects arising from the boundaries. For the same reason obstacles affecting flow are avoided. The trail itself connects the nesting site on the right to a lawn on the left. Regarding the ecological context, ants were not observed to carry any kind of load like nesting material or pieces of prey. Nevertheless the colony was still present for a few more days after data collection.

Probably the most surprising feature is the apparent absence of overtaking. Although ants temporarily left the trail and were passed by succeeding ones, we never observed an ant speeding up in order to overtake. Making use of this observation one is able to extract traffic data based on so-called cumulative counting [23]. Therefore, we use video recordings of the observed section (Fig. 9). Counting itself had to be carried out by hand as various video tracking systems failed. The time of entering and leaving of every single ant is measured. Each ant produces a datapoint for entering ( $t_+^j, n_+^j$ ) and leaving ( $t_-^j, n_-^j$ ) the observed section depending on the direction of movement  $j \in \{L, R\}$ . The  $n$ -th ant enters the section at time  $t_+^j$  and leaves it at time  $t_-^j$ .  $n_+(t)$  ( $n_-(t)$ ) denotes the number of ants that have entered (left) the measurement section up to time  $t$ . The curves defined by the datapoints ( $t_+^j, n_+^j$ ) and ( $t_-^j, n_-^j$ ) are called arrival and departure functions respectively (Fig. 10).

One directly observable quantity is the flow of ants which is given as the slope of the arrival or departure function (Fig. 10 right inset):

$$\Delta t_{\pm}^j(n) = t_{\pm}^j(n) - t_{\pm}^j(n-1) \quad \text{and} \quad f_{\pm}^j(n) = \frac{1}{t_{\pm}^j(n)} \quad (j \in \{L, R\}). \quad (6)$$

Here  $\Delta t_{\pm}(n)$  denotes the time-headway introduced earlier. Under the assumption of approximately constant velocities  $v^j(n)$  (see (8)) along the observed section the distance-headway can be calculated additionally:

$$\Delta d^j(n) = \left( t_+^j(n) - t_+^j(n-1) \right) v^j(n-1) \quad (j \in \{L, R\}) \quad (7)$$

For determining density or average velocity, the length  $L$  of the observed section is needed. By tracing the path of one single ant and putting marks to a transparency on the video screen one obtains  $L$  in units of the body length of the ants. This method avoids errors arising from the observer's perspective or from biasing the trail by direct measurements.

*4.1.2 Derived quantities* As ants do not overtake, the  $n$ -th ant entering is also the  $n$ -th one leaving (Fig. 9 left). Therefore, the average velocity of the  $n$ -th ant while passing the observed section of length  $L$  is given by (Fig. 10 left inset):

$$\langle \Delta T^R(n) \rangle = t_+^R(n) - t_-^R(n) \quad ; \quad \langle v^R(n) \rangle = \frac{L}{\langle \Delta T^R(n) \rangle}. \quad (8)$$

This method in particular makes use of the average velocity rather than of instantaneous measurements. So the measurement is less affected by fluctuations directly observable in the walking speed or direction of movement.

To extract further information about the dependence of traffic flow on the spatial distribution of the ants it is necessary to measure density. Although we will not discuss the fundamental diagram, the method used here has already been employed successfully in case of strictly unidirectional traffic [16].

The instantaneous particle number for one particular direction  $j \in \{L, R\}$  is given by

$$N^j(t) = n_+^j(t) - n_-^j(t) = \text{const.} \quad \text{while} \quad t \in [t_k^j, t_{k+1}^j[; \quad (j \in \{L, R\}). \quad (9)$$

Here  $t_k^j$  denotes the time of an entering or leaving event for one particular direction  $j$ . In both cases the number of ants is changed by one unit. Based on this, one obtains the number of ants  $N^j(t)$  for each direction at a particular instant of time. Since this number is usually not constant during the time a specific ant needs to pass through the observation section, some averaging over the instantaneous particle number  $N^j(t)$  becomes necessary.

Due to the coupling to counterflow also the number of counterflowing ants has to be taken into account. Generally, the total time-evolution of the trail occupation is given by a list  $M$  of entering or leaving events for both directions:

$$M = \{t_i\} \quad \text{with} \quad t_i \in \{t_k^R, t_k^L\}. \quad (10)$$

The elements of  $M$  are sorted by time. The time-average of the instantaneous particle numbers affecting the  $n$ -th ant while passing the observed section (Fig. 10 left inset) is given by

$$\langle N^R(n) \rangle = \frac{A}{\langle \Delta T^R(n) \rangle} \quad \text{with} \quad A = \sum_{t_i=t_+^R(n)}^{t_i < t_-^R(n)} N^R(t_i)(t_{i+1} - t_i), \quad (11)$$

$$\langle N_{cf}^R(n) \rangle = \frac{B}{\langle \Delta T^R(n) \rangle} \quad \text{with} \quad B = \sum_{t_i=t_+^R(n)}^{t_i < t_-^R(n)} N^L(t_i)(t_{i+1} - t_i). \quad (12)$$

Here the average particle number affecting a right moving ant is calculated and therefore the left moving ants are treated as counterflow (Fig. 10 left inset). The instantaneous particle numbers for each direction are averaged from the time of entering  $t_+^R(n)$  to the time of leaving  $t_-^R(n)$  of the  $n$ -th right moving ant. To facilitate comparison with the proposed models, we introduce dimensionless densities by

$$\rho^R(n) = \frac{L}{\langle N^R(n) \rangle} \quad \text{and} \quad \rho_{cf}^R(n) = \frac{L}{\langle N_{cf}^R(n) \rangle}. \quad (13)$$

In case of  $\rho^{cf}(n) < 1$  the travel time  $\langle \Delta T^R(n) \rangle$  is assigned to the unidirectional case and to the bidirectional case otherwise.

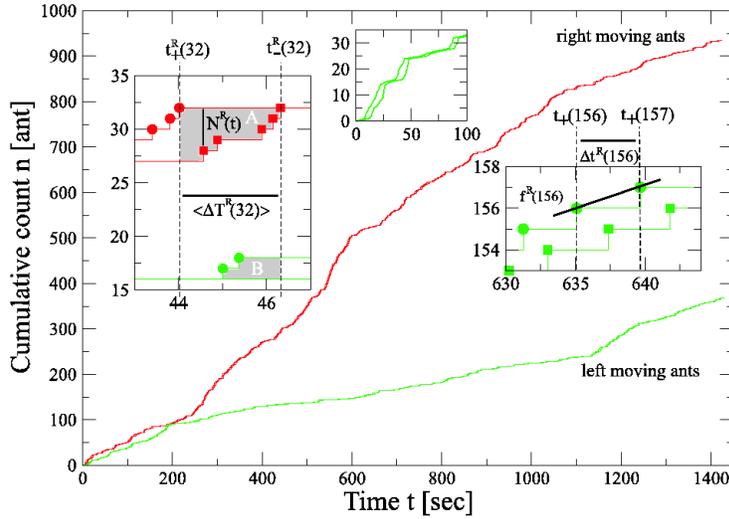


**Fig. 10** Illustration of data extraction. Entering  $n(t_+^R)$  and leaving  $n(t_-^R)$  ants produce datapoints. Based on these, travel time  $\langle \Delta T^R(n) \rangle$  and average velocity  $\langle v^R(n) \rangle$  are calculated. Also the instantaneous number of ants  $N^R(t)$  within the observed section is extracted (see left inset). Based on time headway inflow  $f_+^R(n)$  is calculated (see right inset). Generally, datapoints for entering and leaving ants exhibit a pairwise structure (see middle inset).

#### 4.2 Empirical results

We already made use of some of the qualitative results. Those are also reflected in the quantitative measurements validating the employed methods. The first one is the apparent absence of overtaking. Therefore one finds a pairwise structure of datapoints of entering and leaving ants (see Fig. 10 middle inset). Overall, the departure function is roughly equivalent to the arrival function shifted by the average travel time. Obviously, the time headways are not changed much while passing the observed section. This indicates stable distance-headways (see 7) which will also be subject of subsequent investigations. In case of strictly unidirectional traffic this feature is a consequence of ants moving in platoons, and can easily be observed directly [16].

**4.2.1 Measuring flow** The dominance of flow of right moving ants can be observed directly on the trail and is also indicated by the slope of the corresponding arrival and departure functions (see Fig. 10). For  $t \in [0, 225]$  s flow

in both directions is nearly the same. Starting from  $t \approx 225$  s the flow of right moving ants increases whereas the flow of left moving ants decreases. Starting from  $t \approx 1100$  s, flows are again nearly the same. One behavioral pattern that affects data-collection directly are so-called U-turns. The average rate for right moving ants is about 4% for the first two time-intervals and reaches 7% for the last one. Left moving ants performed U-turns constantly at a rate of about 7%. As flow in both directions is quite fluctuating this might indicate that U-turns are performed independently of flow itself. The existence of U-turns has also consequences for the data analysis since the pairwise structure of datapoints required by the introduced method of measuring average single-ant velocities has to be restored.

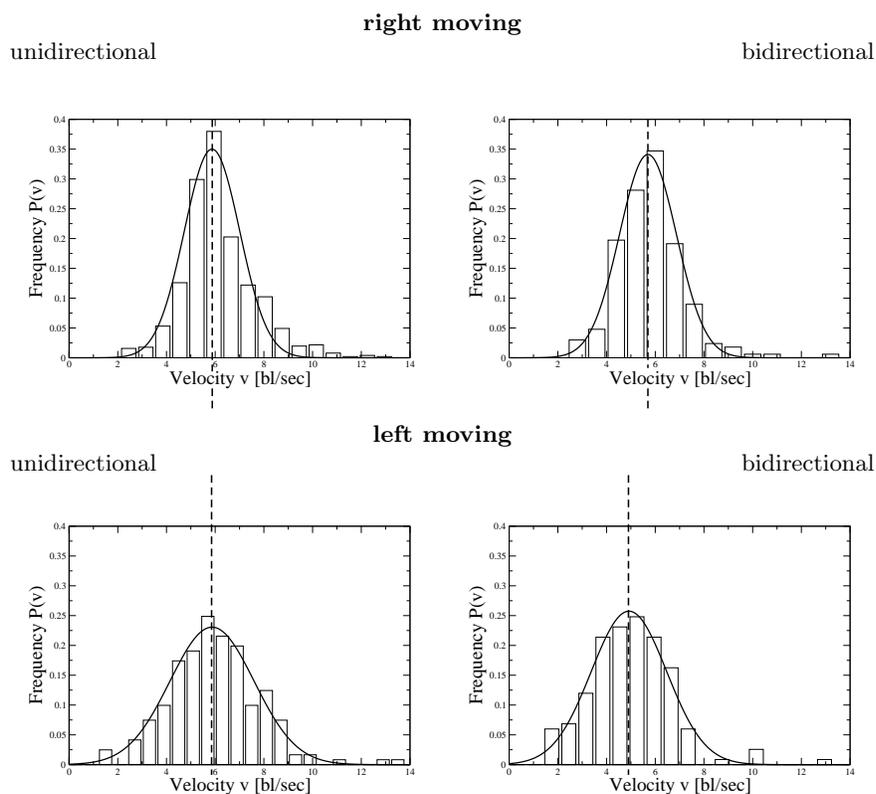


**Fig. 11** Velocity distributions for a real bidirectional single lane trail. The velocity of the right moving ants is hardly affected by counterflow. Average velocity as well as variance are nearly the same in both cases. Additionally, the mean value of left moving ants in absence of counterflow is nearly the same as for right moving ants. But in presence of counterflow a significant decrease is found. Generally one also observes a larger variance for left moving ants.

*4.2.2 Velocity- and distance-headway distributions* For the time-interval of data collection we extracted average velocities according to (8). In order to investigate the impact of counterflow we employ velocity distributions rather than fundamental diagrams. Although those can also be calculated using the described setup, a very large number of datapoints in comparison to the unidirectional case is needed. One would have to cover the whole  $\rho_L \times \rho_R$ -plane instead of the one-dimensional  $\rho$ -line. As a first observation, one finds that the velocity distributions of the right moving ants exhibits a much lower variance than for the left moving ones (see Fig. 9 right). Also the average velocity shows no significant decrease in case of counterflow. This is quite different for the left moving ants. Obviously, the average velocity is significantly decreased by counterflow due to the right moving ants. Overall, one finds two velocities: the reduced one for left moving ants due to counterflow and the second one attained by all right moving ants and for the unidirectional case of the left moving ones. This can be explained by making use of the advantage of employing video recordings for data extraction. Head-on encounters are observed for both directions (see Fig. 9 right). But additionally the right moving ants take advantage of some kind of follow-the-leader behavior. They are occupying the center of the trail. As a consequence, left moving ants move off-center also in absence of counterflow. Therefore the left moving ants are more affected by counterflow. But also generally variance is much larger for left moving ants. This might be caused by the lower density in this direction as a density dependence of the velocity distribution has been found for strictly unidirectional trails [16]. From the videos one observes that the movement of the left moving ants is slightly less directed than for the right moving ants. Therefore a more fluctuating movement is observed. This could be a consequence of the direct connection between trail pheromones and mass orientation known from many other species [15,13].

Also the directly observable spatial pattern are affected as indicated by the distribution of distance-headways (see Fig. 12). Distances between left moving ants are randomly distributed exhibiting a so-called negative exponential distribution. In traffic engineering ([23]) this corresponds to a homogeneous spatial distribution of cars on the road. With respect to our models we therefore find the equivalent of the TASEP-regime (see Fig. 3 left). For the right moving ants generally an asymmetric distribution of distance-headways appears to be more appropriate. This indicates a deviation from the homogeneous spatial distribution found for the left moving ants.

## 5 Summary and discussion

We have introduced two minimal cellular automaton models for traffic on uni- and bi-directional ant trails. Similarities and differences between these models and the models for vehicular traffic or pedestrians dynamics have

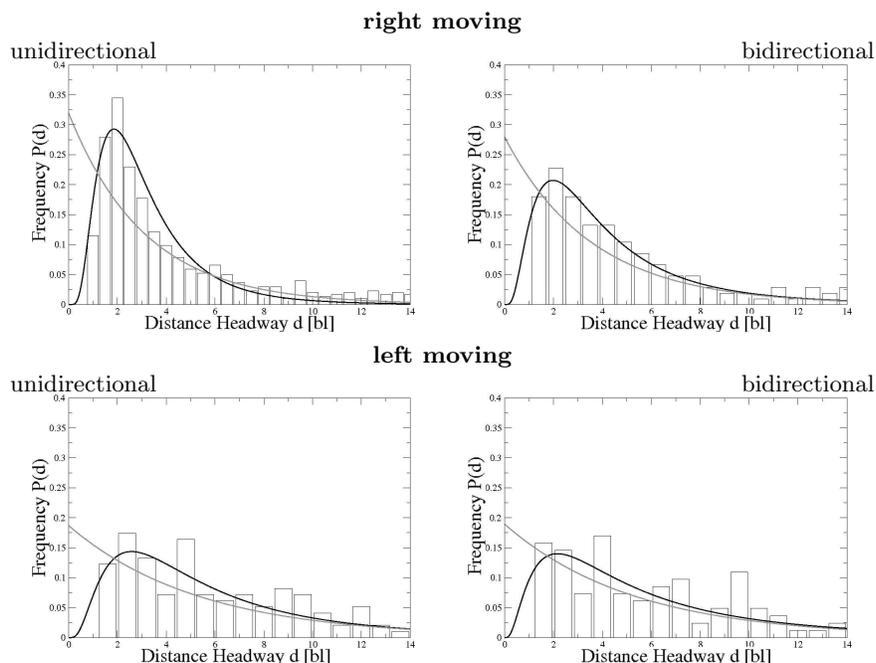


**Fig. 12** Distance-headway distributions for a real bidirectional single lane trail. The left moving ants are distributed homogeneously along the trail. So distance-headways exhibit a negative-exponential distribution (grey). The right moving ants show a different spatial pattern. Obviously an asymmetric distribution of distance-headways (e.g. log-normal) is more appropriate (black).

been emphasized. Especially for pedestrian dynamics there are several similarities which also are supported by recent experiments (see e.g. [27] and references therein). The main interaction in both ant-traffic models is based on different kinds of dynamically induced disorder. In the unidirectional case disorder is assigned to the moving agents by a virtual pheromone field. Although this is quite speculative (as, to our knowledge, no empirical evidence for such an interaction has been found yet), the main feature of the model is quite robust. Probably most other mechanisms, which assign particle-wise disorder with respect to the hopping rates, would produce nearly the same pattern. For the bidirectional model dynamically induced effective site-wise disorder is the key mechanism. This mechanism is independent of the pheromone field as ants moving in counterdirection induce a change in the hopping rates (from  $q$  or  $Q$  to  $K$ ). So this mechanism is based on the directly observable behavior exemplified in Sec. 4.2.

The stationary state in both models is characterized by the spatio-temporal distribution of ants on the trail. We have shown that the flow properties of the system are directly linked to empirically observable aggregation patterns. In particular, the bidirectional model shows a rich variety

of patterns. Based on the general properties of the bidirectional model, we have also pointed out qualitative features of additional quantities which might be of interest in case of bidirectional flow and could also be tested experimentally.

In addition to the investigation of theoretical models, we have presented empirical data obtained by a simple experimental setup. First observations for one particular species *Leptogenys processionalis* at least qualitatively confirm the spatio-temporal patterns predicted by the models [16] (see Fig. 6). In general, clustering phenomena seem to be a common feature in ant colonies [13]. On a quantitative level, velocity distributions and fundamental diagrams have been obtained [4,16]. Also here the main features of the unidirectional model have been found. For the full bidirectional case only few experimental data are available until now [21,4]. Although, in principle, the employed setup is capable of obtaining the full bidirectional fundamental diagram, more data are needed. Therefore, we have restricted the discussion to velocity- and distance-headway distributions for investigating the impact of counterflow. It turns out that in the case of strongly asymmetric flow, as observed here, ants move differently depending on the direction. With respect to our models we would need to introduce different hopping rates for each direction. Nevertheless, the mutual slowing down, as predicted by the models, could be confirmed. Also the impact of counterflow on the spatial distribution of ants along the trail was shown.

The empirically as well as the theoretically observed organization of traffic flow raises fundamental questions on the advantage of such organizations. Both cellular automata models produce moving clusters for an appropriate choice of parameters. In the unidirectional model this happens for a relatively wide density regime. The existence of these clusters corresponds to the regime of constant average velocity. In the TASEP the average velocity decreases strictly monotonically with increasing density as ants are distributed homogeneously along the trail. So moving in clusters enables the ants to keep on moving at a higher velocity in comparison with a homogeneous distribution in TASEP. This is obviously achieved by reducing mutual blocking. One might argue that the fundamental diagram shows a maximum value of average velocity. This maximum is attained at the point of sharp increase from the cluster- to the homogeneous distribution. Nevertheless, a maximum of the average velocity at this point would be quite unstable. Even small fluctuations in density would lead to large fluctuations in the average velocity. In comparison, the cluster regime is quite stable against fluctuations in density. Therefore, in natural systems clustering is expected to lead to a decrease of travel time which can be seen as a user optimum.

In the bidirectional case, moving clusters only occur at very low densities. The underlying mechanism is still the same as in the unidirectional model. At intermediate to high densities the main feature, namely the formation of localized clusters leading to a constant value of flow, emerges. This feature solely depends on the presence of counterflow. In this situation flow is the crucial quantity. In an appropriate ecological context, the

outbound flow for example determines the number of ants travelling to the food source, whereas inbound flow is related to the amount of food carried back to the nest. Very different values of inbound and outbound flow would lead to a too large or too small number of ants at the source. So a vanishing effective flow, which is roughly independent of density fluctuations, also ensures a constant number of workers at a particular destination. As this feature involves flow, it can be interpreted as some kind of system optimum.

## Acknowledgments

The authors would like to thank M. Burd, P. Chakroborty, R. Gadagkar, B. Hölldobler, A. Kunwar and T. Varghese for informative discussions. They also thank the referees and the editor for helpful suggestions concerning the presentation. Parts of the presented work of one of the authors (AJ) has been supported by the German Academ through a joint Indo-German research project.

## References

1. Bonabeau, E., Dorigo, M., Theraulaz, G. (1999). *Swarm Intelligence: From natural to artificial systems*. New York: Oxford University Press.
2. Bonabeau, E., Dorigo, M., Theraulaz, G. (2000). Inspiration for optimization from social insect behaviour. *Nature*, 406, 39.
3. Burd, M. (2006). Ecological consequences of traffic organisation in ant societies. *Physica A*, 372, 124.
4. Burd, M., Archer, D., Aranwela, N., Stradling, D. J. (2002). Traffic dynamics of the leaf-cutting ant. *Atta cephalotes*. *American Naturalist*, 159, 283.
5. Chopard, B., Droz, M. (1998). *Cellular automata modelling of physical systems*. Cambridge: Cambridge University Press.
6. Chowdhury, D., Santen, L., Schadschneider, A. (2000). Statistical physics of vehicular traffic and some related systems. *Physics Reports*, 329, 199.
7. Chowdhury, D., Guttal, V., Nishinari, K., Schadschneider, A. (2002). A cellular-automata model of flow in ant-trails: Non-monotonic variation of speed with density. *Journal of Physics A: Mathematical and General*, 35, L573.
8. Chowdhury, D., Nishinari, K., Schadschneider, A. (2004). Self-organized patterns and traffic flow in colonies of organisms: from bacteria and social insects to vertebrates. *Phase Transition*, 77, 601.
9. Couzin, I. D., Franks, N. R. (2003). Self-organized lane formation and optimized traffic flow in army ants. *Proceedings of Royal Society London B*, 270, 139.
10. Dussutour, A., Fourcassié, V., Helbing, D., Deneubourg, J.-L. (2004). Optimal traffic organization in ants under crowded conditions. *Nature*, 428, 70.
11. Dussutour, A., Deneubourg, J.-L., Fourcassié, V. (2005). Temporal organisation of bi-directional traffic in the ant *Lasius niger* (1). *Journal of Experimental Biology*, 208, 2903.
12. Dussutour, A., Beshers, S., Deneubourg, J.-L., Fourcassié, V. (2007). Crowding increases foraging efficiency in the leaf-cutting ant. *Atta Colombica*. *Insectes Sociaux*, 54, 168.

13. Hölldobler, B., Wilson, E. O. (1990). *The ants*. Cambridge: The Belknap Press of Harvard University Press.
14. Howard, J. (2001). *Mechanics of motor proteins and the cytoskeleton*. Sunderland: Sinauer Associates.
15. Jackson, D. E., Ratnieks, F. L. W. (2006). Communication in ants. *Current Biology*, 16, R570.
16. John, A. (2006). *Physics of traffic on ant trails and related systems*. Ph.D. thesis, Universität zu Köln, Germany.
17. John, A., Schadschneider, A., Chowdhury, D., Nishinari, K. (2004). Collective effects in traffic on bidirectional ant-trails. *Journal of Theoretical Biology*, 231, 279.
18. Krug, J., Ferrari, P. A. (1996). Phase transitions in driven diffusive systems with random rates. *Journal of Physics A*, 29, L465.
19. John, A., Kunwar, A., Namazi, A., Chowdhury, D., Nishinari, K., Schadschneider, A. (2007a). Traffic on bidirectional ant-trails. In N. Waldau, P. Gattermann, H. Knoflacher, M. Schreckenberg (Eds.), *Pedestrian and evacuation dynamics 2005* (pp. 465). Berlin: Springer.
20. John, A., Kunwar, A., Namazi, A., Schadschneider, A., Chowdhury, D., Nishinari, K. (2007b). Traffic on bi-directional ant-trails: Coarsening behaviour and fundamental diagrams. In A. Schadschneider, T. Pöschel, R. Kühne, M. Schreckenberg, D.E. Wolf (Eds.), *Traffic and granular flow 05* (pp. 269). Berlin: Springer.
21. Johnson, K., Rossi, L. F. (2006). A mathematical and experimental study of ant foraging line dynamics. *Journal of Theoretical Biology*, 241, 360.
22. Kunwar, A., John, A., Nishinari, K., Schadschneider, A., Chowdhury, D. (2004). Collective traffic-like movement of ants on a trail: dynamical phases and phase transitions. *Journal of Physical Society of Japan*, 73, 2979.
23. May, A. D. (1990). *Traffic flow fundamentals*. Englewood Cliffs: Prentice Hall.
24. Moffet, M. W. (1987). Ants that go with the flow: A new method of orientation by mass communication. *Naturwissenschaften*, 74, 551.
25. Nagel, K., Schreckenberg, M. (1992). A cellular automaton model for freeway traffic. *Journal of Physics I France*, 2, 2221.
26. Schadschneider, A., Kirchner, A., Nishinari, K. (2003). From ant trails to pedestrian dynamics. *Applied Bionics and Biomechanics*, 1, 11.
27. Schadschneider, A., Klingsch, W., Klüpfel, H., Kretz, T., Rogsch, C., Seyfried, A. (2008). Evacuation dynamics: Empirical results, modeling and applications. In Meyers B. (Ed.), *Encyclopedia of complexity and system science*. New York: Springer.
28. Schütz, G. M. (2000). Exactly solvable models for many-body systems far from equilibrium. In C. Domb, J.L. Lebowitz (Eds.), *Phase transitions and critical phenomena* (Vol. 19). London: Academic Press.
29. Tripathy, G., Barma, M. (1997). Steady state and dynamics of driven diffusive systems with quenched disorder. *Physics Review Letters*, 78, 3039.